

# Directional Direct Feedback Alignment: Estimating Backpropagation Paths for Efficient Learning on Neural Processors

Florian Bacho and Dominique Chu

**Abstract**—The error Backpropagation algorithm (BP) is a key method for training deep neural networks. While performant, it is also resource-demanding in terms of computation, memory usage and energy. This makes it unsuitable for online learning on edge devices that require a high processing rate and low energy consumption. More importantly, BP does not take advantage of the parallelism and local characteristics offered by dedicated neural processors. There is therefore a demand for alternative algorithms to BP that could improve the latency, memory requirements, and energy footprint of neural networks on hardware. In this work, we propose a novel method based on Direct Feedback Alignment (DFA) which uses Forward-Mode Automatic Differentiation to estimate backpropagation paths and learn feedback connections in an online manner. We experimentally show that Directional DFA achieves performances that are closer to BP than other feedback methods on several benchmark datasets and architectures while benefiting from the locality and parallelization characteristics of DFA. Moreover, we show that, unlike other feedback learning algorithms, our method provides stable learning for convolution layers.

## I. INTRODUCTION

In the past decades, the error Backpropagation algorithm (BP) [1] has developed into an indispensable technique to train Deep Neural Networks (DNNs) with high performance. However, BP has numerous drawbacks. First, it relies on the sequential propagation of errors through layers which hinders the ability to parallelise the backward pass and inherently slows down the gradient computation [2]. Secondly, the transposes of the weights of downstream layers are needed to compute errors of hidden neurons. This requires costly data movement and increases the hardware energy consumption during training [3], [4]. Finally, BP requires saving many intermediate results during inference for the backward pass, leading to high memory usage [3], [2].

Training DNNs is computationally expensive and requires high amounts of energy. To address this, massively-parallel dedicated neural processors can be designed to take advantage of the parallel aspect of neural circuits [5], [6], [7], [2], [3], [8], [9]. Such hardware relies on data reuse and locality to avoid costly transport of information and to optimize power efficiency. Neural processors offer numerous advantages that can substantially reduce the energy footprint of DNNs and decrease the latency of data processing. This is especially beneficial in edge devices where energy consumption, computation time and privacy are major challenges. [10]. However, the non-local characteristics of BP make it unsuitable for efficient online learning on dedicated neural processors [2], [3] and

alternatives to BP are needed to optimize the speed, energy efficiency and memory usage of training on hardware [4].

Motivated by this, several local alternatives to BP have been proposed. These include unsupervised learning methods such as Deep Infomax [11] and Greedy InfoMax [12] that optimize the mutual information of each layer in the network. Other techniques like synthetic gradients [13] sidestep error backpropagation by creating decoupled neural interfaces that predict gradients or local error signals that define local layer-wise loss functions [14], [15]. Another alternative to BP is Random Feedback Alignment (FA) [16]. It uses random feedback matrices during the backward pass to create a propagation path dissociated from the forward weights which removes the need for weight transport.

The Random Direct Feedback Alignment (DFA) algorithm takes the idea of FA one step further by directly projecting output errors to hidden layers using fixed linear random feedback connections [17], [18], [3], [2], [4]. Since the backward computation only relies on linear projections of output errors and local gradients, DFA enables the efficient parallelization of the backward pass or *backward unlocking* [17], [4]. DFA also demonstrates improved training speed and lower energy consumption on dedicated neural processors compared to BP [8]. However, even though DFA easily scales to modern deep learning architectures such as Transformers [18], [2], [4], a performance gap exists with BP which increases with the complexity of the task and becomes catastrophic when DFA is applied to Convolutional Neural Networks (CNNs) [2], [19], [20].

One possible approach to improve the performance of FA is to learn feedback connections. Examples are methods like weight mirroring [21] and the Kolen-Pollack algorithms [21], [19]. These algorithms adapt feedback connections by either learning the transpose of weights or reciprocally adjusting feedbacks according to the changes of forward weights [21], [19]. Feedback learning provides improved alignment between forward and feedback weights, leading to better descending directions as well as higher performance compared to fixed random connections. However, weight mirroring and the Kolen-Pollack algorithm require fine hyperparameter balance to be stable [22] and suffer from gradient explosion when used on CNNs without Batch Normalization (BN) [19]. To the best of our knowledge, only the Kolen-Pollack method has been adapted as a DFA algorithm, henceforth referred to as Direct Kolen-Pollack (DKP) [19].

To improve DFA, we conjecture that feedback connections

are ideal when they approximate the partial derivatives of outputs with respect to hidden neurons. Based on this assumption, we introduce a novel algorithm that uses Forward-Mode Automatic Differentiation (Forward-Mode AD) to estimate backpropagation paths and learn feedback connections in an entirely online manner. Our main contributions are:

- 1) We describe how directional derivatives evaluated in random directions can be used to estimate backpropagation paths from outputs to hidden neurons during inference and propose a corresponding feedback learning rule for DFA. The resulting algorithm, *Directional DFA*, benefits from backward unlocking of DFA while learning feedbacks in an online manner without having to perform backpropagation.
- 2) We show that, unlike DKP, Directional DFA does not suffer from gradient explosion when used on CNNs and is capable of training shallow CNNs even without the help of batch normalization.
- 3) We scale Directional DFA to deep convolutional architectures (AlexNet) and benchmark on CIFAR100 to determine whether our method can solve the failure of Random DFA to train deep CNNs. We show that our method significantly improves performance compared to Random DFA but that even when feedbacks approximate backpropagation paths, DFA still fails to train deep CNNs as a gap with BP remains. However, we show that transfer learning allows closing this gap and that Directional DFA still performs the best among DFA methods.

## II. BACKGROUND

In this section, we briefly review the backpropagation algorithm to highlight the causes of backward locking and describe several concepts that are used in our Directional DFA method.

### A. Deep Neural Network

Let  $L$  be the depth of a Deep Neural Network and  $n_l$  the number of neurons in the layer  $l$ . We denote by  $\mathbf{y}_0 \in \mathbb{R}^{n_0}$  the inputs of the network,  $W^{(l)} \in \mathbb{R}^{n_l \times n_{l-1}}$  the weights matrix defining the synaptic strengths between the layer  $l$  and its preceding  $l-1$ . The outputs  $\mathbf{y}^{(l)}$  of the layer  $l$  are thus defined as follows:

$$\mathbf{a}^{(l)} = W^{(l)} \mathbf{y}^{(l-1)}, \quad \mathbf{y}^{(l)} = \sigma(\mathbf{a}^{(l)}) \quad (1)$$

where  $\mathbf{a}^{(l)}$  are the preactivations of the layer and  $\sigma(x)$  is a pointwise differentiable activation function. We will thus denote by  $\sigma'(x)$  its first order derivative,  $\frac{\partial \sigma(x)}{\partial x}$ .

### B. Error Backpropagation

We now briefly review the error backpropagation algorithm.

Given any differentiable loss function  $\mathcal{L}$ , the weight gradient of the layer  $l$  is defined by all the partial derivatives of  $\mathcal{L}$  with respect to the weights, such as:

$$\frac{\partial \mathcal{L}}{\partial w_{ij}^{(l)}} = \delta_i^{(l)} \frac{\partial y_i^{(l)}}{\partial w_{ij}^{(l)}} \quad (2)$$

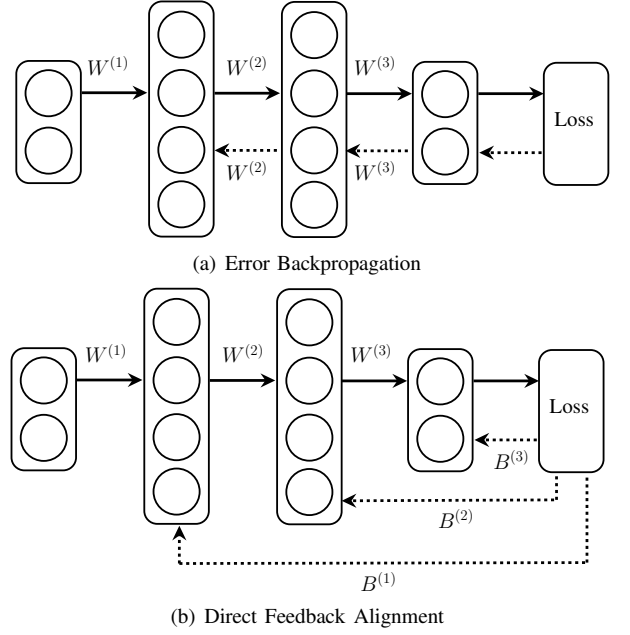


Fig. 1. Illustrations of the error backpropagation (Figure 1(a)) and Direct Feedback Alignment (Figure 1(b)). Solid arrows represent forward paths and dotted arrows represent backpropagation paths.

where

$$\delta_i^{(l)} := \sum_{o=1}^{n_L} \frac{\partial \mathcal{L}}{\partial y_o^{(L)}} \frac{\partial y_o^{(L)}}{\partial y_i^{(l)}} \quad (3)$$

is the error associated with the neuron,  $\frac{\partial \mathcal{L}}{\partial y_o^{(L)}}$  is the error signal at the outputs, provided by the loss module, and

$$\frac{\partial y_i^{(l)}}{\partial w_{ij}^{(l)}} = \sigma'(a_i^{(l)}) y_j^{(l-1)} \quad (4)$$

is the local partial derivative that only depends on information directly available to the neuron, i.e. inputs, pre-activation and activation.

For output neurons,  $\delta_i^{(L)}$  is simply equal to the error signal as no backpropagation is required. For hidden neurons, errors are sequentially backpropagated from downstream layers using the chain rule, such as:

$$\delta_i^{(l)} = \begin{cases} \frac{\partial \mathcal{L}}{\partial y_o^{(L)}} & \text{if } l = L \\ \sum_{k=1}^{n_{l+1}} \frac{\partial y_k^{(l+1)}}{\partial y_i^{(l)}} \delta_k^{(l+1)} & \text{if } l < L \end{cases} \quad (5)$$

Equation 5 shows the cause of backward locking in BP. To compute errors of specific hidden neurons, the computation of downstream's neurons errors is required. This sequential propagation during the backward pass locks the computation of layers' gradients and limits the parallelization of BP. To solve this problem, new approaches have been proposed such as the Direct Feedback Alignment algorithm.

### C. Direct Feedback Alignment

In Direct Feedback Alignment (DFA) [17], the partial derivatives  $\frac{\partial y_o^{(L)}}{\partial y_i^{(l)}}$  in Equation 3 are replaced by fixed linear feedback

connections. in this way, DFA sidesteps error backpropagation as the computation of the chain rule in Equation 5 is avoided by linearly projecting errors from output to hidden neurons. Figure 1 shows a comparative illustration of BP and DFA. By denoting  $B^{(l)} \in \mathbb{R}^{n_l \times n_L}$  as the feedback matrix that replaces the backpropagation paths between the outputs and the hidden layers  $l$ , the error  $\bar{\delta}_i^{(l)}$  received by the neurons  $i$  can be written as follows [17]:

$$\bar{\delta}_i^{(l)} = \sum_{o=1}^{n_L} \frac{\partial \mathcal{L}}{\partial y_o^{(L)}} b_{io}^{(l)} \quad (6)$$

For the output layer, the feedback matrix  $B^{(L)}$  is set as the identity matrix. The gradient of the output layer is thus identical to BP as errors are directly available and no error projection or backpropagation is required. For hidden layers, feedback connections are commonly chosen to be fixed random matrices. In this case, the method is referred as *Random DFA* [17]. Learning with random feedbacks can seem counter-intuitive. However, DNNs can align their weights with the feedbacks, thus aligning their gradients with the true gradients. If the approximate gradient lies within  $90^\circ$  of the true gradient, it thus provides a descending direction for small enough learning rates [16], [17], [20].

#### D. Forward-Mode Automatic Differentiation

Contrary to Reverse-Mode Automatic Differentiation (AD) which constructs a computational graph and requires backward evaluations to compute gradients, Forward-Mode AD simultaneously computes functions and directional derivatives in a completely forward way [23], [24], [25].

Let  $f(\mathbf{w})$  be a function of parameters  $\mathbf{w}$ . Using Forward-Mode AD simultaneously computes  $f(\mathbf{w})$  and the directional derivative  $d_{\mathbf{v}}f(\mathbf{w})$  evaluated in a given direction  $\mathbf{v}$ , such as:

$$d_{\mathbf{v}}f(\mathbf{w}) = \nabla f(\mathbf{w}) \mathbf{v} = \sum_{i=1}^n \frac{\partial f(\mathbf{w})}{\partial w_i} v_i \quad (7)$$

where  $\nabla f(\mathbf{w})$  is the true gradient of  $f$  evaluated at  $\mathbf{w}$ .

The directional derivative  $d_{\mathbf{v}}f(\mathbf{w})$  is a scalar representing the rate of change of  $f$  along the direction  $\mathbf{v}$  when evaluated at  $\mathbf{w}$ . Geometrically, scaling the given direction  $\mathbf{v}$  by the directional derivative  $d_{\mathbf{v}}f(\mathbf{w})$  gives the projection of the gradient  $\nabla f(\mathbf{w})$  at  $\mathbf{w}$  onto  $\mathbf{v}$  – see Figure 2(a).

In Forward Mode AD,  $\mathbf{v}$  is usually set with a one-hot vector to compute the exact partial derivative with respect to a single parameter. If  $\mathbf{v}$  is a one hot vectors with all elements set to 0 except for the element  $j$  that is set to 1, Equation 7 becomes:

$$d_{\mathbf{v}}f(\mathbf{w}) = \frac{\partial f(\mathbf{w})}{\partial w_j} \quad (8)$$

To compose a full gradient,  $n$  directional derivatives must be computed with  $n$  one hot vector corresponding to each element of  $\mathbf{w}$ . Therefore, this requires  $n$  forward differentiation to obtain the full gradient which is more computationally expensive than Reverse-Mode AD, especially when the number of parameters is large as in DNNs [25].

#### E. Directional Gradient

An alternative to the use of one-hot vectors in Forward Mode AD has been independently proposed in [24] and [25]. Instead of evaluating the directional derivative in the direction of a single parameter at a time using a one-hot vector, the directional derivative  $d_{\mathbf{v}}f(\mathbf{w})$  is evaluated in a random direction  $\mathbf{v} \sim \mathcal{N}(\mathbf{0}, \mathbf{I})$  following a multivariate standard normal distribution. The directional gradient (also called forward gradient in [25]) is therefore defined by the product  $d_{\mathbf{v}}f(\mathbf{w})\mathbf{v}$  between the directional derivative  $d_{\mathbf{v}}f(\mathbf{w}, \mathbf{v})$  and the direction vector  $\mathbf{v}$ .

Because of the nature of  $\mathbf{v}$ , we can demonstrate that the expected directional gradient  $\mathbb{E}[d_{\mathbf{v}}f(\mathbf{w})\mathbf{v}]$  is an unbiased estimation of the true gradient  $\nabla f(\mathbf{w})$  when averaged over many different random directions [24], [25]. Each element  $i$  of the expected directional gradient can be decomposed as follows:

$$\begin{aligned} \mathbb{E}[d_{\mathbf{v}}f(\mathbf{w})v_i] &= \sum_{j=1}^n \frac{\partial f(\mathbf{w})}{\partial w_j} v_j v_i \\ &= \frac{\partial f(\mathbf{w})}{\partial w_i} \mathbb{E}[v_i^2] + \sum_{j \neq i} \frac{\partial f(\mathbf{w})}{\partial w_j} \mathbb{E}[v_i v_j] \end{aligned} \quad (9)$$

As each element  $v_i$  follows a normal distribution of mean 0 and variance 1,  $\mathbb{E}[v_i] = 0$  and  $\mathbb{E}[v_i^2] = \mathbb{E}[v_i] + \text{Var}[v_i] = 1$ . Therefore, Equation 9 reduces to the partial derivative with respect to  $w_i$ :

$$\begin{aligned} \mathbb{E}[g_i(\mathbf{w}, \mathbf{v})] &= \frac{\partial f(\mathbf{w})}{\partial w_i} \\ \Leftrightarrow \mathbb{E}[\mathbf{g}(\mathbf{w}, \mathbf{v})] &= \nabla f(\mathbf{w}) \end{aligned} \quad (10)$$

Figure 2(b) illustrates the expected directional gradient.

However, this method does not perform as well as backpropagation and DFA [24], [25] because the averaging process requires a large number of random directions.

### III. METHOD

In this section, we motivate and describe the iterative feedback learning rule that underpins Directional DFA.

#### A. Feedback Connections Represent Backpropagation Paths

To improve DFA, we are interested in learning feedback connections instead of using fixed random weights. Equation 6 shows that the feedback matrix  $B$  replaces the backpropagation paths in Equation 3, represented by the partial derivatives of the outputs with respect to the hidden neurons. Unlike partial derivatives in BP, feedback connections in DFA are not sample-dependent as they are used for every training sample. We are thus working with the heuristics that an ideal feedback connection  $b_{io}^{(l)}$  between the output neuron  $o$  and the hidden neuron  $i$  in layer  $l$  would work best if it approximates the partial derivative  $\frac{\partial y_o^{(L)}}{\partial y_i^{(l)}}$  for all the samples of the training dataset, such as:

$$b_{io} = \mathbb{E} \left[ \frac{\partial y_o^{(L)}}{\partial y_i^{(l)}} \right] \quad (11)$$

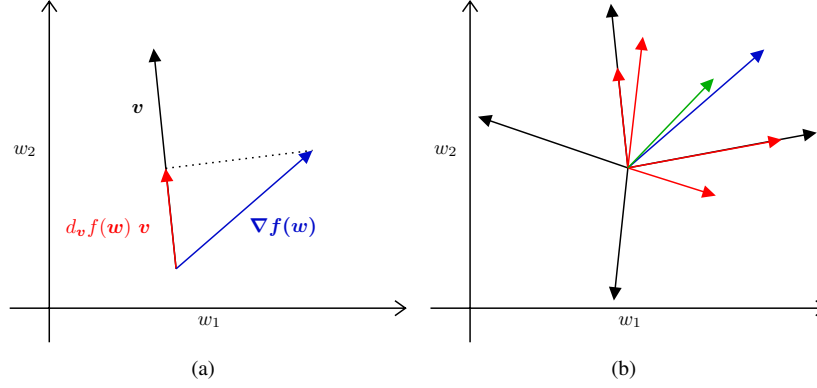


Fig. 2. Figure 2(a): Projection of the gradient  $\nabla f(w)$  at  $w$  onto a given direction  $v$ . The vector  $d_v f(w) v$  is obtained by scaling the direction  $v$  by the directional derivative  $d_v f(w)$  evaluated at  $w$  in the direction of  $v$ . Figure 2(b): The expected directional derivative (green arrow), computed by averaging directional gradients (red arrows) over many random directions (black arrows), is an unbiased estimate of the true gradient (blue arrow).

Reverse-Mode AD could be used to compute the expected partial derivatives over the dataset. However, computing Equation 11 using Reverse-Mode AD is impractical when the dataset contains a large number of samples or in online learning where data is not available at all times. Additionally, Reverse-Mode AD is inefficient, non-local and leads to backward locking. We thus propose an alternative method to estimate these expected partial derivatives in a fully online manner by using Forward-Mode AD.

### B. Estimating Backpropagation Paths

One way to compute gradients while avoiding the limitations of Reverse-Mode AD is to use Forward-Mode AD, as described in [24] and [25]. In this method, directions are randomly drawn for each weight of the network which are used to estimate the gradient using Forward-Mode AD. In Directional DFA, we take a different approach. Rather than directly estimating the full gradient, we estimate the expected backpropagation paths as described by Equation 11. By sampling random directions for the output of each hidden neuron in the network, we can use Forward-Mode AD to estimate the partial derivatives of the output of the network with respect to the hidden neurons in an online manner. In the following, we thus show how this applies to a DNN. We denote by  $v^{(l)} \in \mathbb{R}^{n_l}$  the direction vector for each layer of the network. For each hidden layer  $l$ , we draw  $v^{(l)} \sim \mathcal{N}(0, I)$  from a multivariate normal distribution. For input and output neurons, the direction vectors  $v^{(0)}$  and  $v^{(L)}$  respectively are set to 0 as they do not require differentiation. Using Forward-Mode AD we then compute the directional derivative  $d_i^{(l)}$  associated with the neuron  $i$  of layer  $l$ :

$$d_i^{(l)} := \sum_{j=1}^{n_{l-1}} \frac{\partial y_i^{(l)}}{\partial y_j^{(l-1)}} d_j^{(l-1)} + v_i^{(l)} \quad (12)$$

The first term on the right-hand side of Equation 12 applies the chain rule to the directional derivatives of upstream neurons to perform first-order differentiation. The second term corresponds to the drawn direction which allows differentiation in downstream neurons. Note that Equation 12 only contains

**Algorithm 1** Directional Direct Feedback Alignment algorithm on a feedforward DNN. Here, the operator  $\odot$  corresponds to the Hadamard product.

---

**Input:** Training data  $D = \{x_s\}_{s=1}^M$   
 Randomly initialize  $w_{ij}^{(l)}$  for all  $l, i$  and  $j$ .  
 Initialize  $b_{io}^{(l)} = 0$  for all  $l, i$  and  $o$ .  
**repeat**  
 {Inference (sequential)}  
**for**  $s = 1$  **to**  $M$  **do**  
 $y^{(0)} \leftarrow x_s$   
 $d^{(0)} \leftarrow 0$   
**for**  $l = 1$  **to**  $L$  **do**  
 Sample  $v^{(l)} \sim \mathcal{N}(0, I)$   
 $a^{(l)} \leftarrow W^{(l)} y^{(l-1)}$   
 $y^{(l)} \leftarrow f(a^{(l)})$   
 $d^{(l)} \leftarrow (W^{(l)} d^{(l-1)}) \odot \sigma'(a^{(l)}) + v^{(l)}$   
 $G^{(l)} \leftarrow \sigma'(a^{(l-1)}) y^{(l-1)T}$   
**end for**  
 $e \leftarrow \frac{\partial \mathcal{L}}{\partial y^{(L)}}$   
 {Weights and feedbacks updates (parallel)}  
**for**  $l = 1$  **to**  $L$  **do**  
 $\nabla W^{(l)} \leftarrow G^{(l)} \odot (B^{(l)} e)$   
 $\nabla B^{(l)} \leftarrow B^{(l)} - (v^{(l)} d^{(L)T})$   
 $W^{(l)} \leftarrow W^{(l)} - \lambda \nabla W^{(l)}$   
 $B^{(l)} \leftarrow B^{(l)} - \alpha \nabla B^{(l)}$   
**end for**  
**end for**  
**until**  $\mathcal{L} < \epsilon$

---

locally available information and can therefore be computed in an online manner along with the forward pass.

After the inference, a directional derivative  $d_o^{(L)}$  is produced along with the activation of each output neuron  $o$ . Each directional derivative represents the rates of change of the output  $o$  in the direction:

$$d_o^{(L)} = \sum_{l=1}^{L-1} \sum_{j=1}^{n^{(l)}} \frac{\partial y_o^{(L)}}{\partial y_j^{(l)}} v_j^{(l)} \quad (13)$$

Following [24], [25] we can show that the products between the output directional derivatives and the drawn directions are, on average, unbiased estimates of the expected backpropagation paths described by Equation 11:

$$\begin{aligned}\mathbb{E} \left[ d_o^{(L)} v_i^{(l)} \right] &= \mathbb{E} \left[ \sum_{l'=1}^{L-1} \sum_{j=1}^{n^{(l')}} \frac{\partial y_o^{(L)}}{\partial y_j^{(l')}} v_j^{(l')} v_i^{(l)} \right] \\ &= \sum_{l'=1}^{L-1} \sum_{j=1}^{n^{(l')}} \mathbb{E} \left[ \frac{\partial y_o^{(L)}}{\partial y_j^{(l')}} \right] \mathbb{E} \left[ v_j^{(l')} v_i^{(l)} \right] \\ &= \mathbb{E} \left[ \frac{\partial y_o^{(L)}}{\partial y_i^{(l)}} \right]\end{aligned}\quad (14)$$

as

$$\mathbb{E} \left[ v_j^{(l')} v_i^{(l)} \right] = \begin{cases} 0 & \text{if } l' \neq l \text{ and } i \neq j \\ 1 & \text{if } l' = l \text{ and } i = j \end{cases} \quad (15)$$

Therefore, this estimate can be used as a feedback connection to directly project errors from the output neuron  $o$  onto the hidden neurons  $i$  of layer  $l$ , such as:

$$b_{io} = \mathbb{E} \left[ d_o^{(L)} v_i^{(l)} \right] \quad (16)$$

Computing the expectation in Equation 16 is still impractical due to the averaging over the entire dataset as well as many random directions. Moreover, this estimate becomes obsolete as the network weights are updated which induces changes in the partial derivatives. To relax the computational cost of this estimate and to allow adaptation to weight updates, we define a learning rule for the feedback that implements a moving average of  $d_o^{(L)} v_i^{(l)}$  over the past sample evaluations, such as:

$$b_{io}^{(l)} \leftarrow b_{io}^{(l)} + \alpha \left( d_o^{(L)} v_i^{(l)} - b_{io}^{(l)} \right) \quad (17)$$

where  $0 < \alpha < 1$  is the feedback learning rate.

To be able to use more complex optimization techniques such as Adam [26], we can define a feedback gradient as follows:

$$\nabla b_{io}^{(l)} := b_{io}^{(l)} - d_o^{(L)} v_i^{(l)} \quad (18)$$

and update feedbacks with gradient descent:

$$b_{io}^{(l)} \leftarrow b_{io}^{(l)} - \alpha \nabla b_{io}^{(l)} \quad (19)$$

Algorithm 1 summarizes the full algorithm applied to a fully-connected DNN.

We have now defined a rule to update the feedback matrices. Based on the results in [24] and [25] discussed above, we expect that the feedback matrices will, over time, approach the expected partial derivatives described by Equation 11 and thus lead to better performing learning in DFA. Note that all computation relies only on Forward-Mode AD which is entirely performed in an online manner without backpropagation. Moreover, Equation 17 only requires locally-available information such as the output directional derivative, the draw direction of the hidden neuron and the feedback itself. Therefore, the proposed feedback update is a local learning rule that does not require any transport of information.

## IV. RESULTS

We conducted several experiments to measure the improvements of the proposed approach over random DFA and DKP. We first trained DNNs with different depth as well as CNNs on MNIST [27], FashionMNIST [28] CIFAR10 and CIFAR100 [29] and report average test performances for comparison. Secondly, we trained again each network with Batch Normalization (BN) to measure the impact on performance. Finally, we compare the gradient alignment between each DFA method and the true gradient provided by BP to measure the quality of the weight updates.

### A. Experimental Settings

In our experiments, we trained three fully-connected DNNs with an increasing number of hidden layers (1, 2 and 3 hidden layers) on every dataset. Additionally, we trained a CNN with the following architecture: 15C5-P2-40C5-P2-128-10 where 15C5 represents 15 5x5 convolutional layers and P2 represents a 2x2 max pooling layer. For CIFAR100, we used the AlexNet architecture [30] and up-scaled images to 224x224. Each network was trained 10 times with BP, random DFA, DKP and our Directional DFA algorithms. We used the following set of hyperparameters for training.

All the inputs were normalized to lie between -1 and 1. No data augmentation was applied except for CIFAR100 where a random crop was used. We used a ReLU activation function and a cross-entropy loss for every layer except for the outputs that remained linear. For random DFA, the weights and biases were initialized to zero, as suggested in [16], [17], while the feedback matrices were initialized with the uniform Kaiming initialization [31]. For DKP and our directional DFA algorithm, the feedback matrices were initialized to zero while forward weights were initialized with uniform Kaiming. We trained the networks with a batch size of 64 for every dataset except for AlexNet on CIFAR100 where a batch size of 128 was used. Training was performed during 100 epochs using Adam [26] with  $\beta_1 = 0.9$ ,  $\beta_2 = 0.999$ ,  $\epsilon = 10^{-8}$  and a learning rate  $\lambda = 10^{-4}$ . A learning rate of  $\lambda = 5 \times 10^{-4}$  was used for the shallow CNNs. We also used Adam for feedback learning with a learning rate of  $\alpha = 10^{-4}$  in both DKP and directional DFA. For DKP, both forward and feedback weights decay factors were set to  $10^{-6}$ . In every training, we used a learning rate scheduler for the forward learning rate  $\lambda$  with a decay factor of 0.95 applied at the end of each epoch.

### B. Performance Comparison

Table II and I summarizes the testing performances of all methods with and without batch normalization respectively. Here, BP performances are given as references and random DFA, DKP and our Directional DFA are compared.

First of all, we observe that random DFA suffers from performance degradation compared to BP which is consistent with previous work [17], [2], [19]. This accuracy gap becomes more important when the network contains convolutional layers, even if the network only contains a few convolutional layers.

TABLE I

PERFORMANCE COMPARISON OF BP, RANDOM DFA, DKP AND DIRECTIONAL DFA ON THE MNIST, FASHION MNIST AND CIFAR10 DATASETS WITH DIFFERENT NETWORK ARCHITECTURES **WITHOUT** BATCH NORMALIZATION. THE PERFORMANCE OF BP IS GIVEN AS A REFERENCE AND ONLY DFA METHODS ARE COMPARED. BEST PERFORMANCES BETWEEN RANDOM DFA, DKP AND DIRECTIONAL DFA ARE GIVEN IN BOLD. 3x800 MEANS A NETWORK ARCHITECTURE OF 3 FULLY-CONNECTED LAYERS OF 800 NEURONS. *Conv* REFERS TO THE SHALLOW CNN.

DATASET	ARCH	BP	RANDOM DFA	DKP	DIR. DFA
MNIST	1x800	$98.25 \pm 0.04\%$	$98.04 \pm 0.07\%$	$98.12 \pm 0.05\%$	<b><math>98.21 \pm 0.02\%</math></b>
	2x800	$98.39 \pm 0.06\%$	$98.18 \pm 0.06\%$	$98.28 \pm 0.06\%$	<b><math>98.3 \pm 0.04\%</math></b>
	3x800	$98.46 \pm 0.05\%$	$98.15 \pm 0.05\%$	$98.27 \pm 0.05\%$	<b><math>98.32 \pm 0.05\%</math></b>
	CONV	$99.32 \pm 0.03\%$	$98.8 \pm 0.08\%$	$98.62 \pm 0.13\%$	<b><math>99.16 \pm 0.03\%</math></b>
FASHION MNIST	1x800	$89.37 \pm 0.09\%$	$88.67 \pm 0.12\%$	$89.09 \pm 0.11\%$	<b><math>89.27 \pm 0.07\%</math></b>
	2x800	$90.01 \pm 0.08\%$	$89.19 \pm 0.13\%$	$89.63 \pm 0.12\%$	<b><math>89.82 \pm 0.13\%</math></b>
	3x800	$89.99 \pm 0.15\%$	$89.15 \pm 0.09\%$	$89.48 \pm 0.09\%$	<b><math>89.56 \pm 0.11\%</math></b>
	CONV	$92.1 \pm 0.16\%$	$89.69 \pm 0.22\%$	$86.21 \pm 1.28\%$	<b><math>91.54 \pm 0.11\%</math></b>
CIFAR10	1x1000	$56.2 \pm 0.12\%$	$54.8 \pm 0.22\%$	$55.41 \pm 0.18\%$	<b><math>55.74 \pm 0.14\%</math></b>
	2x1000	$56.66 \pm 0.18\%$	$54.2 \pm 0.11\%$	$55.15 \pm 0.24\%$	<b><math>55.7 \pm 0.15\%</math></b>
	3x1000	$56.92 \pm 0.19\%$	$53.61 \pm 0.16\%$	$54.35 \pm 0.21\%$	<b><math>54.97 \pm 0.19\%</math></b>
	CONV	$68.11 \pm 0.57\%$	$58.14 \pm 0.94\%$	$41.02 \pm 2.63\%$	<b><math>66.96 \pm 0.70\%</math></b>

TABLE II

PERFORMANCE COMPARISON OF BP, RANDOM DFA, DKP AND DIRECTIONAL DFA ON THE MNIST, FASHION MNIST, CIFAR10 AND CIFAR100 DATASETS WITH DIFFERENT NETWORK ARCHITECTURES **WITH** BATCH NORMALIZATION. \* TRANSFER LEARNING WAS USED BY PRE-TRAINING CONVOLUTION LAYERS AND FREEZING THEM DURING THE TRAINING OF THE FULLY-CONNECTED LAYERS.

DATASET	ARCH	BP	RANDOM DFA	DKP	DIR. DFA
MNIST	1x800	$98.28 \pm 0.05\%$	$98.19 \pm 0.05\%$	<b><math>98.3 \pm 0.04\%</math></b>	$98.26 \pm 0.03\%$
	2x800	$98.58 \pm 0.06\%$	$98.41 \pm 0.06\%$	$98.39 \pm 0.05\%$	<b><math>98.52 \pm 0.06\%</math></b>
	3x800	$98.7 \pm 0.06\%$	$98.46 \pm 0.04\%$	$98.5 \pm 0.06\%$	<b><math>98.63 \pm 0.05\%</math></b>
	CONV	$99.4 \pm 0.05\%$	$99.22 \pm 0.05\%$	$99.23 \pm 0.04\%$	<b><math>99.44 \pm 0.03\%</math></b>
FASHION MNIST	1x800	$90.12 \pm 0.12\%$	$90.0 \pm 0.11\%$	$90.08 \pm 0.1\%$	<b><math>90.09 \pm 0.1\%</math></b>
	2x800	$90.43 \pm 0.08\%$	$90.05 \pm 0.14\%$	$89.92 \pm 0.13\%$	<b><math>90.16 \pm 0.14\%</math></b>
	3x800	$90.87 \pm 0.14\%$	$89.95 \pm 0.1\%$	$90.05 \pm 0.11\%$	<b><math>90.25 \pm 0.12\%</math></b>
	CONV	$91.86 \pm 0.19\%$	$90.86 \pm 0.11\%$	$91.46 \pm 0.19\%$	<b><math>92.12 \pm 0.1\%</math></b>
CIFAR10	1x1000	$56.72 \pm 0.23\%$	$56.11 \pm 0.18\%$	$56.51 \pm 0.18\%$	<b><math>56.55 \pm 0.17\%</math></b>
	2x1000	$57.32 \pm 0.19\%$	$56.04 \pm 0.22\%$	$55.89 \pm 0.23\%$	<b><math>56.56 \pm 0.32\%</math></b>
	3x1000	$58.11 \pm 0.29\%$	$55.57 \pm 0.34\%$	$55.63 \pm 0.21\%$	<b><math>56.6 \pm 0.19\%</math></b>
	CONV	$69.85 \pm 0.36\%$	$62.76 \pm 0.57\%$	$65.66 \pm 0.97\%$	<b><math>69.34 \pm 0.54\%</math></b>
CIFAR100	ALEXNET	$66.72 \pm 0.28\%$	$48.92 \pm 0.55\%$	$56.56 \pm 0.37\%$	<b><math>57.04 \pm 0.22\%</math></b>
	ALEXNET*	$66.94 \pm 0.04\%$	$66.09 \pm 0.14\%$	$66.45 \pm 0.11\%$	<b><math>66.60 \pm 0.21\%</math></b>

Compared to random DFA, DKP generally performs better on all tasks and architectures. These improvements are attributed to the greater alignment provided by the Kolen-Pollack feedback learning, as described in [19]. However, a performance gap still exists with BP.

The accuracy degradation seen in both random DFA and DKP is less important with the proposed Directional DFA method. Performances achieved by our approach are closer to BP than the other benchmarked methods on most of the tasks and architectures. It is thus clear that the proposed Directional DFA algorithm generally outperforms both random DFA and DKP.

### C. Impact of Batch Normalization

Batch Normalization (BN) [32] is widely used in today's DNNs. BN normalizes values of pre-activations to reduce internal covariate shift and facilitate training [32]. The use of BN thus is known to improve the convergence speed and performance of DNNs. A drawback of BN is that it is memory and computationally expensive and strongly depends on the batch size which could be an obstacle to on-chip online learning.

It has been reported in [19] that DKP suffers from gradient explosion when BN is not used before the activation. During our experiments, we found that our method successfully trains

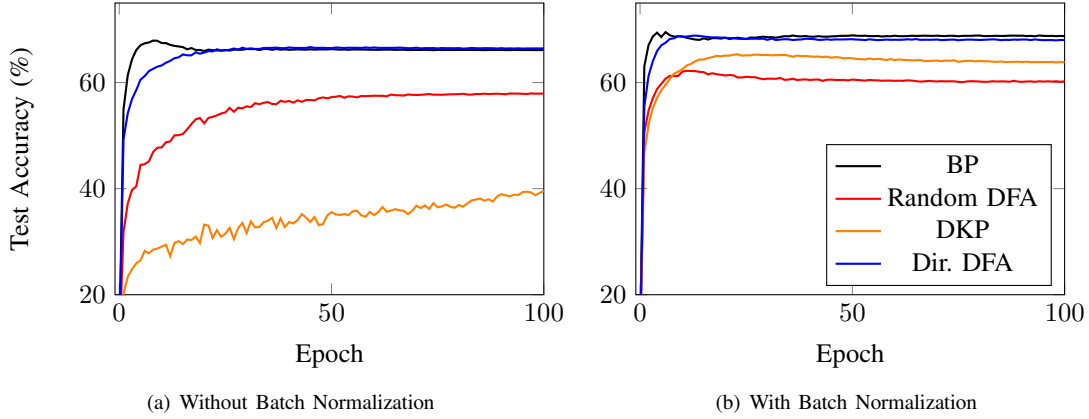


Fig. 3. Evolution of the test accuracy of the CNN trained with BP (black), random DFA (red), DKP (orange) and Directional DFA (blue) on CIFAR10 without BN (Figure 3(a)) and with BN (Figure 3(b)).

CNNs without BN. We thus report the test accuracies with and without BN for all architectures in Table II and I respectively. BN globally improves convergence speed and test performance of all methods. However, even though DKP successfully trains fully-connected networks without BN, it fails to train CNNs and performs worse than random DFA. Figure 3 shows the evolution of the test accuracies of CNNs with and without BN trained with the benchmarked methods on CIFAR10. We can observe that the model without BN trained with DKP fails to converge properly while Random and Directional DFA converges smoothly. Therefore, CNNs trained with our method are capable of learning without the help of BN which offers advantages in terms of memory, computation cost and online learning.

#### D. Deep Convolutional Networks

DFA is known to fail on Deep CNNs [2], [33], [4], [19]. To evaluate the scalability of each method on deep CNNs, we trained a network with the AlexNet architecture [30] on CIFAR100. Results were reported in Table II. BP achieves an average test performance of 66.72%. However, Random DFA fails to train AlexNet properly as it only reaches 48.92% of accuracy. Both DKP and our Directional DFA improve performances compared to Random DFA as they achieve 56.56% and 57.04% respectively, with a slight advantage for Directional DFA. Despite the improvements made by feedback learning, performances remain far from BP suggesting that the methods also fail to learn useful features in deeper layers. To confirm this assumption, we pre-trained AlexNet using BP and applied transfer learning [34] by freezing the convolution layers and training the 3-layers classifier using each method. As shown in Table II, transfer learning brings performances of all DFA methods close to BP, confirming that DFA fails to train deep convolutional feature extractors even when feedbacks approximate backpropagation paths. Despite the increase in performance of every method, Directional DFA remains the approach that performs best among all DFA methods.

#### E. Gradient Alignment

We now quantify the quality of the gradient provided by each DFA method. An approximate gradient that has a direction close to the true gradient can minimize the loss function faster than an approximate gradient that points away from the minima. Therefore, to better understand how our approach compares to other DFA methods, we measured the gradient alignment of both methods during training of a 6-layer fully-connected DNN with BN on MNIST. More precisely, we measured the layerwise angle between the approximate and the gradient provided by BP using the cosine distance metric:

$$C(\nabla_{\mathbf{W}^{(l)}}, \hat{\nabla}_{\mathbf{W}^{(l)}}) = \frac{180}{\pi} \arccos \left( \frac{\nabla_{\mathbf{W}^{(l)}} \hat{\nabla}_{\mathbf{W}^{(l)}}}{\|\nabla_{\mathbf{W}^{(l)}}\| \|\hat{\nabla}_{\mathbf{W}^{(l)}}\|} \right) \quad (20)$$

where  $\nabla_{\mathbf{W}^{(l)}}$ ,  $\hat{\nabla}_{\mathbf{W}^{(l)}}$  are respectively the flattened true and approximate gradients of layer  $l$ .

Figure 4 shows the layerwise gradient alignment comparison of the trained DNN for each method. As expected from feedback learning, the approximate gradient produced by the DKP is more aligned with the true gradient than random DFA. However, the improvement is minor compared to the proposed Directional DFA. Our method produces approximate gradients that are closer to the true gradients than the ones produced by random DFA and DKP. This suggests that the quality of the Directional DFA gradient is greater than other DFA methods and that our method is capable of converging faster towards minimas.

#### F. Computational Cost and Hardware Efficiency

We consider here the computational cost and hardware efficiency of each method. First of all, Random DFA decreases the computational cost of training as no backpropagation is performed. This benefits hardware efficiency as only errors have to be transported and allows backward unlocking for faster weight updates and leads to improved energy consumption [8].

Both DKP and the proposed Directional DFA have a higher computational cost than Random DFA due to the additional feedback learning rule. Therefore, energy consumption would



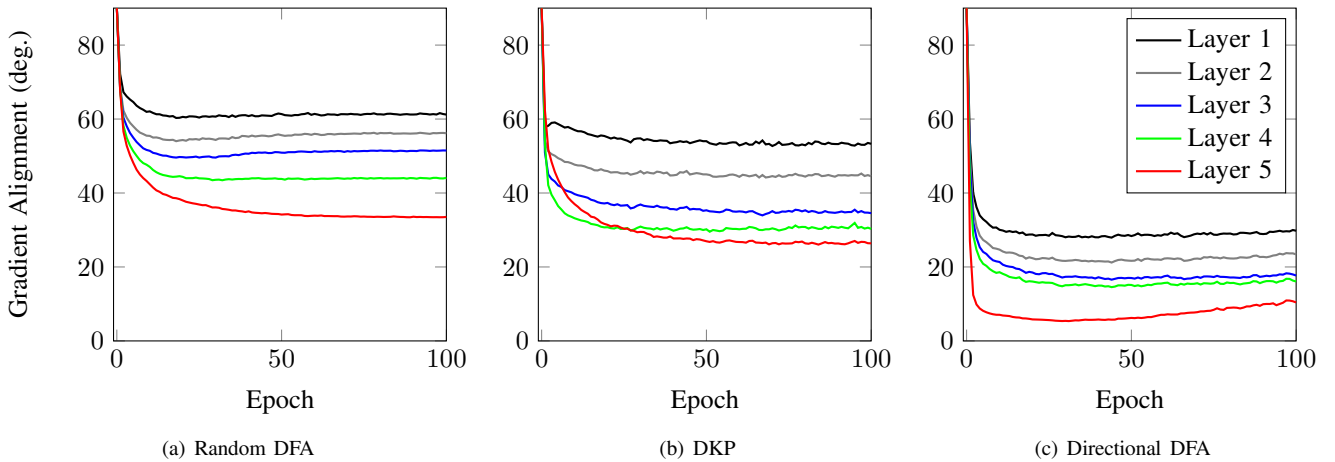


Fig. 4. Layerwise alignment between the approximate gradient provided by each method and the true gradient provided by BP. The angles are here given in degree and lower values mean better alignment. Directional DFA provides improved descending directions compared to random DFA and DKP as the layerwise alignment angles are significantly lower.

increase when implemented on hardware because of the additional memory writes that would be required to update feedbacks. In Directional DFA, directional derivatives are computed along with forward activations which double the amount of Multiply-Accumulate (MAC) operations required to perform matrix multiplications. Directional DFA is therefore the most computationally expensive DFA method during inference but data reuse would be possible on hardware as the method relies on locally-available information.

Conversely, BP does not take advantage of data reuse. Many intermediate results have to be stored in memory for backpropagation and global data movements are required [3]. As the majority of the energy consumption of dedicated neural processors comes from read and write from off-chip DRAM rather than MAC operations, BP is inherently limited in how energy efficient it can be made [35], [3]. In contrast, Directional DFA benefits from less transport of information. Consequently, we can expect Directional DFA to be more energy efficient than BP on appropriate hardware as the cost of data movement is higher than the cost of MAC operations [35], [3].

## V. DISCUSSION

In this work, we proposed a novel algorithm to learn feedback connections in DFA based on Forward-Mode AD. By evaluating directional derivatives in random directions, Directional DFA provides an unbiased estimate of the expected backpropagation paths as feedbacks. As Forward-Mode AD is performed along with the network’s forward pass and takes advantage of data reuse, our method would benefit from fewer data movements than BP and thus reduced energy consumption if implemented on suitable hardware. Moreover, because gradients rely on locally-available information as well as linearly projected error signals, the gradient computation does not require sequential propagation as in BP. Therefore, this unlocks the backward pass and allows weight updates to be performed entirely in parallel which reduces the computation

time of training and allows increased data processing rate on hardware [2].

In our experiments, we demonstrated that Directional DFA outperforms other DFA methods trained on MNIST, Fashion MNIST, CIFAR10 and CIFAR100 with both feedforward and convolutional neural networks, thus achieving performances that are closer to BP. We showed that, unlike the DKP algorithm, Directional DFA also achieves stable training on convolution layers without the use of batch normalization. As BN requires full batches to compute the mean and variance of its inputs, it can be an obstacle to online learning where data samples are only available one at a time. Therefore, our method offers a better advantage for on-the-edge online learning than DKP.

We also observed that, like every other DFA method, Directional DFA still fails to train deep CNNs even if backpropagation paths are approximated. This empirically confirms previous findings that there is no general choice of feedbacks that allows alignment in convolution layers due to their constrained structure and their lack of flexibility [33], [20]. To overcome this limitation, it is common to use transfer learning [8], [4]. We showed that our approach also outperforms other DFA methods using transfer learning.

In terms of computational cost, using fixed random feedback matrices is the least computationally expensive method for training DNNs with DFA. It has been shown [2], [8] that dedicated neural processors that implement random DFA improve training speed (by a factor of 2) as well as energy-efficiency (by more than 35%) compared to hardware that is optimized for BP. We expect that the equivalent improvements for DKP and Directional DFA would be more modest. The reason for this is that feedback connections also need to be updated which would require additional circuitry. Moreover, the number of MAC operations required by Directional DFA during training is double compared to other methods as first-order differentiation has to be performed along with neuron activations. Therefore, Directional DFA would be the most expensive DFA method to implement on hardware. However,



the amount of external memory access would remain lower than BP as most of the computation in Directional DFA takes advantage of data reuse. Hence the energy consumption of MAC operations is insignificant compared to external memory access [35], [3], [8], we expect our approach to be more energy-efficient than BP while providing better performance than other DFA methods.

## VI. CODE AVAILABILITY

The code produced in this work will be made available at: <https://github.com/Florian-BACHO/DirDFA>

## REFERENCES

- [1] D. E. Rumelhart and J. L. McClelland, *Learning Internal Representations by Error Propagation*, 1987, pp. 318–362.
- [2] D. Han and H.-j. Yoo, “Direct feedback alignment based convolutional neural network training for low-power online learning processor,” in *2019 IEEE/CVF International Conference on Computer Vision Workshop (ICCVW)*, 2019, pp. 2445–2452.
- [3] B. Crafton, A. Parihar, E. Gebhardt, and A. Raychowdhury, “Direct feedback alignment with sparse connections for local learning,” *Frontiers in neuroscience*, vol. 13, p. 525, 2019.
- [4] J. Launay, I. Poli, F. Boniface, and F. Krzakala, “Direct feedback alignment scales to modern deep learning tasks and architectures,” in *Proceedings of the 34th International Conference on Neural Information Processing Systems*, ser. NIPS’20. Red Hook, NY, USA: Curran Associates Inc., 2020.
- [5] Y.-H. Chen, T. Krishna, J. S. Emer, and V. Sze, “Eyeriss: An energy-efficient reconfigurable accelerator for deep convolutional neural networks,” *IEEE journal of solid-state circuits*, vol. 52, no. 1, pp. 127–138, 2016.
- [6] C. Li, D. Belkin, Y. Li, P. Yan, M. Hu, N. Ge, H. Jiang, E. Montgomery, P. Lin, Z. Wang *et al.*, “Efficient and self-adaptive in-situ learning in multilayer memristor neural networks,” *Nature communications*, vol. 9, no. 1, pp. 1–8, 2018.
- [7] D. Bankman, L. Yang, B. Moons, M. Verhelst, and B. Murmann, “An always-on 3.8μJ/86% cifar-10 mixed-signal binary cnn processor with all memory on chip in 28nm cmos,” *2018 IEEE International Solid - State Circuits Conference - (ISSCC)*, pp. 222–224, 2018.
- [8] D. Han, J. Lee, J. Lee, and H.-J. Yoo, “A 1.32 tops/w energy efficient deep neural network learning processor with direct feedback alignment based heterogeneous core architecture,” in *2019 Symposium on VLSI Circuits*, 2019, pp. C304–C305.
- [9] M. Osta, M. Alameh, H. Younes, A. Ibrahim, and M. Valle, “Energy efficient implementation of machine learning algorithms on hardware platforms,” 11 2019.
- [10] M. Zhang, F. Zhang, N. D. Lane, Y. Shu, X. Zeng, B. Fang, S. Yan, and H. Xu, *Deep Learning in the Era of Edge Computing: Challenges and Opportunities*. John Wiley & Sons, Ltd, 2020, ch. 3, pp. 67–78.
- [11] D. Hjelm, A. Fedorov, S. Lavoie-Marchildon, K. Grewal, P. Bachman, A. Trischler, and Y. Bengio, “Learning deep representations by mutual information estimation and maximization,” in *ICLR 2019*. ICLR, April 2019.
- [12] S. Löwe, P. O’ Connor, and B. Veeling, “Putting an end to end-to-end: Gradient-isolated learning of representations,” in *Advances in Neural Information Processing Systems*, H. Wallach, H. Larochelle, A. Beygelzimer, F. d’ Alché-Buc, E. Fox, and R. Garnett, Eds., vol. 32. Curran Associates, Inc., 2019.
- [13] M. Jaderberg, W. M. Czarnecki, S. Osindero, O. Vinyals, A. Graves, D. Silver, and K. Kavukcuoglu, “Decoupled neural interfaces using synthetic gradients,” in *International conference on machine learning*. PMLR, 2017, pp. 1627–1635.
- [14] H. Mostafa, V. Ramesh, and G. Cauwenberghs, “Deep supervised learning using local errors,” *Frontiers in Neuroscience*, vol. 12, 2018.
- [15] A. Nøkland and L. H. Eidnes, “Training neural networks with local error signals,” in *Proceedings of the 36th International Conference on Machine Learning*, ser. Proceedings of Machine Learning Research, K. Chaudhuri and R. Salakhutdinov, Eds., vol. 97. PMLR, 09–15 Jun 2019, pp. 4839–4850.
- [16] T. P. Lillicrap, D. Cownden, D. B. Tweed, and C. J. Akerman, “Random synaptic feedback weights support error backpropagation for deep learning,” *Nature Communications*, vol. 7, 2016.
- [17] A. Nøkland, “Direct feedback alignment provides learning in deep neural networks,” in *Advances in Neural Information Processing Systems*, D. Lee, M. Sugiyama, U. Luxburg, I. Guyon, and R. Garnett, Eds., vol. 29. Curran Associates, Inc., 2016.
- [18] D. Han and H.-J. Yoo, “Efficient convolutional neural network training with direct feedback alignment,” *ArXiv*, vol. abs/1901.01986, 2019.
- [19] M. B. Webster, J. Choi *et al.*, “Learning the connections in direct feedback alignment,” 2020.
- [20] M. Refinetti, S. D’Ascoli, R. Ohana, and S. Goldt, “Align, then memorise: the dynamics of learning with feedback alignment,” in *International Conference on Machine Learning*, 2021, pp. 8925–8935.
- [21] M. Akrouf, C. Wilson, P. C. Humphreys, T. Lillicrap, and D. Tweed, *Deep Learning without Weight Transport*. Red Hook, NY, USA: Curran Associates Inc., 2019.
- [22] D. Kunin, A. Nayeibi, J. Sagastuy-Brena, S. Ganguli, J. M. Bloom, and D. L. K. Yamins, “Two routes to scalable credit assignment without weight symmetry,” ser. ICML’20. JMLR.org, 2020.
- [23] C. C. Margossian, “A review of automatic differentiation and its efficient implementation,” *WIREs Data Mining and Knowledge Discovery*, vol. 9, no. 4, p. e1305, 2019.
- [24] D. Silver, A. Goyal, I. Danihelka, M. Hessel, and H. van Hasselt, “Learning by directional gradient descent,” in *International Conference on Learning Representations*, 2021.
- [25] A. G. Baydin, B. A. Pearlmutter, D. Syme, F. Wood, and P. Torr, “Gradients without backpropagation,” 2022.
- [26] D. Kingma and J. Ba, “Adam: A method for stochastic optimization,” *International Conference on Learning Representations*, 12 2014.
- [27] Y. LeCun, C. Cortes, and C. Burges, “Mnist handwritten digit database,” *ATT Labs [Online]*. Available: <http://yann.lecun.com/exdb/mnist>, vol. 2, 2010.
- [28] H. Xiao, K. Rasul, and R. Vollgraf, “Fashion-mnist: a novel image dataset for benchmarking machine learning algorithms,” 2017.
- [29] A. Krizhevsky, “Learning multiple layers of features from tiny images,” 2009.
- [30] A. Krizhevsky, I. Sutskever, and G. E. Hinton, “Imagenet classification with deep convolutional neural networks,” in *Proceedings of the 25th International Conference on Neural Information Processing Systems - Volume 1*, ser. NIPS’12. Red Hook, NY, USA: Curran Associates Inc., 2012, p. 1097–1105.
- [31] K. He, X. Zhang, S. Ren, and J. Sun, “Delving deep into rectifiers: Surpassing human-level performance on imagenet classification,” *2015 IEEE International Conference on Computer Vision (ICCV)*, pp. 1026–1034, 2015.
- [32] S. Ioffe and C. Szegedy, “Batch normalization: Accelerating deep network training by reducing internal covariate shift,” in *Proceedings of the 32nd International Conference on Machine Learning*, ser. Proceedings of Machine Learning Research, F. Bach and D. Blei, Eds., vol. 37. Lille, France: PMLR, 07–09 Jul 2015, pp. 448–456.
- [33] J. Launay, I. Poli, and F. Krzakala, “Principled training of neural networks with direct feedback alignment,” 06 2019.
- [34] S. Bozinovski, “Reminder of the first paper on transfer learning in neural networks, 1976,” *Informatica*, vol. 44, 09 2020.
- [35] H. Kwon, M. Pellauer, and T. Krishna, “Maestro: an open-source infrastructure for modeling dataflows within deep learning accelerators,” *arXiv preprint arXiv:1805.02566*, 2018.